

Increase in Near Surface Temperature Simulation Skill due to Predictive Soil Moisture in a

Numerical Seasonal Simulation under Observed SST Forcing

By

Laurel L. De Haan

And

Masao Kanamitsu

Scripps Institution of Oceanography

University of California, San Diego.

Corresponding author: Laurel DeHaan, Mail Code 0224; CRD/SIO/UCSD; 9500 Gilman Drive; La Jolla, CA 92093-0224
E-mail: ldehaan@ucsd.edu

Abstract

Two sets of 12-year 8-member ensemble integrations were run with the ECPC SFM to investigate the sensitivity of near surface temperature skill to evolving soil moisture. The first ensemble had evolving soil moisture, which was fully interactive with the atmospheric component of the model. The second ensemble had soil moisture fixed to the monthly climatological value. Several regions showed an increase in skill in the evolving soil moisture ensemble, including Northeastern Australia, Southeastern Africa, Europe, Northern Brazil, Western Australia, Northwestern Russia, Argentina, Western Canada, and Indo-China. A survey of these regions showed that most had sensitivity to soil moisture following a peak rainy season and of those, most also had a high soil moisture time-lag correlation (soil moisture memory) at that time. In a few of the regions high year-to-year soil moisture variability was an additional potential source of soil moisture sensitivity.

The sensitivity to soil moisture is considered both in terms of actual predictability (anomaly correlation with observations) and theoretical potential predictability. It was found that the regions listed above, with evolving soil moisture, have anomaly correlations that are close to the potential predictability, suggesting that the model estimates near-surface temperature in these regions as well as could be expected. However, it was found that when comparing the two sets of integrations, improvements in potential predictability of one ensemble over the other do not necessarily give a reasonable estimate to improvements in anomaly correlation.

1. Introduction

In the past several years it has become clear that soil moisture and land surface processes play an important role in climate prediction. While it is well understood that the response of general circulation models to tropical sea surface temperatures (SSTs) is of primary importance to climate prediction, it is apparent that soil moisture has an important secondary role. As a result, there has been an increased interest in understanding the impact of soil moisture on near surface temperature and precipitation in general circulation models (GCMs). The influence of soil moisture is more localized than SSTs (although not completely localized) and accordingly one of the key interests is the location of soil moisture sensitivities. For example, Simmonds and Hope (1998) and Timbal et al (2002) found significant sensitivities to soil moisture in Australia. Yang et al (2004) saw improved anomaly correlations due to soil moisture over the U.S. in summer. Koster et al (2004) looked globally to find the summertime land-atmosphere coupling “hot-spots”, which included the central U.S., Northern India, and equatorial Africa.

While there has been some agreement on areas sensitive to soil moisture, there is also some disagreement. Much of the disagreement is due to model sensitivities in these studies (Koster et al 2002). This disagreement can be seen, for example, in Koster (2004) where 12 models are used to determine land-atmosphere coupling “hot-spots”. Even in these “hot-spots” some models show almost no land-atmosphere coupling strength. It is also unclear what the best method is to determine the degree of sensitivity to soil moisture. There have been a few different methods used to address this question. Many papers have looked at soil moisture initialization (e.g. Fennessy and Shukla 1999, Zhang and Frederiksen 2003, Koster and Suarez 2003, and Kanamitsu et al 2003), while others have focused on soil moisture forcing. Of the papers concerned with forcing, some have forced a model with “observed” soil moisture looking for improved results (e.g. Dirmeyer 2000, Yang 2004, and Kanae et al 2006), while others used a non-varying soil moisture (e.g. Oglesby et al 2002, Douville 2003, and Koster et al 2004) purely to assess soil moisture sensitivity. Many papers have used a theoretical measure such as

potential predictability or a ratio of variances (e.g. Schlosser and Milly 2002, Timbal et al 2002, Oglesby et al 2002, Douville 2003, and Koster 2004), while a few have included anomaly correlations against observations as an element of the measure of sensitivity to soil moisture (e.g. Yang et al 2004 and Kanae et al 2006). Many have forced the GCMs with observed SSTs (e.g. Douville 2003 and Kanae et al 2006), while others used prescribed SSTs without interannual variability (e.g. Schlosser and Milly 2002).

Here we look at the impact of interactive soil moisture on the actual predictability measure of anomaly correlation against observations as well as the theoretical measure of potential predictability. While it is likely that there are remote influences of soil moisture, we primarily consider the local effects here. We consider two-month averages at regions around the globe using a GCM forced with observed SSTs. After discussing the model and experiment (sections 2 and 3), we examine selected regions to answer the questions of how much and where the real predictability (skill) is increased by including the soil moisture component into the forecast system. The regions with soil moisture sensitivity are evaluated not only in terms of anomaly correlation and potential predictability, but also in terms of precipitation annual cycle, soil moisture memory, and soil moisture variability with the intent of understanding the potential sources of soil moisture sensitivity. In section 5, we examine the relationship between the real model skill and potential predictability, first by looking at the fully interactive ensemble alone, and then by looking at the differences between the two ensembles for the two skill measures. This is done in an effort to address the applicability of the potential skill to real skill, which is essential for real time seasonal forecasts.

2. Model

The Experimental Climate Prediction Center's (ECPC's) seasonal forecast model (SFM) is used for this study (Kanamitsu et al 2002). It has a horizontal resolution of T62 with 28 vertical levels. The model has relaxed Arakawa-Schubert convection, M-D Chou short and long

wave radiation (Chou and Lee 1996, Chou and Suarez 1994), Slingo cloud scheme (Slingo, 1987), shallow convection (Tiedtke, 1983), large scale condensation, gravity wave drag (Alpert et al 1988) and smoothed mean orography. The current version of the SFM has been upgraded to include the Noah land surface model (LSM) (Ek et al 2003). This LSM includes four sub-surface levels and frozen soil physics. Soil moisture is computed using a form of Richardson's equation. The LSM has 16 soil types and 12 vegetation types. Vegetation cover is a monthly varying climatology.

The performance of this version of the model has been fully examined in a 53-year ensemble AMIP type simulation. We have run a 12-member ensemble with observed SSTs (AMIP type) from 1949 to 2001. The model skill under observed SSTs and evolving soil moisture is comparable to other seasonal forecast models in operation in the U.S. Particularly, the precipitation forecast over Africa, and most notably the Sahel, is found to be exceptional among the models used in the operational multi-model ensemble forecast at the International Research Institute (IRI). A 50-year anomaly correlation of precipitation in the Sahel shows correlations greater than 0.7 in some areas (Tippett, 2006). As an example of the model two-meter temperature skill, Figure 1 shows the anomaly correlation computed from the AMIP type run and verified against CRU temperature (Climatic Research Unit in the University of Norwich, United Kingdom <http://www.cru.uea.ac.uk/>) for summertime (JJA). The skill shown here is at a minimum typical of what would be found in most state-of-the-art GCMs, and in some locations, such as Australia and Indonesia, it is notably high. Based on its performance in all seasons, the ECPC SFM has been used since 2002 to produce a seasonal forecast every month at the ECPC, which is used in the IRI multi-model forecast, as well as by other forecasters.

3. Experiment

To look at the effects of soil moisture on the skill of the forecast in a realistic setup, two sets of ensembles were integrated with the ECPC SFM. Both ensembles were run continuously

for 12 years, from 1982-1993 in order to include three El Niño events. Both ensembles had eight members, where each member was initialized with slightly different atmospheric initial conditions. The interactive ensemble is a subset of the 53-year AMIP run and was initialized in 1949 from reanalysis data, and the climatological ensemble was initialized in 1982 from the interactive ensemble. Both ensembles were also forced with observed SSTs (AMIP-style). This allows a reasonable estimate of how much the soil moisture information adds skill to model forecasts with specified SSTs. The question we are asking is whether the predictable part of the signal generated by the observed SSTs can be enhanced by the land surface conditions, and whether the soil moisture can add predictability on top of the SSTs, although we cannot attempt to separate them.

The first ensemble has evolving soil moisture (i.e. a fully interactive land surface model). This ensemble will be referred to as the interactive ensemble. The second ensemble was run with climatological soil moisture. While each member was initialized with different atmospheric initial conditions, it was forced with the same climatological soil moisture. The monthly soil moisture climatologies were created from the 53-year AMIP-style run with the same model. This method allowed the soil moisture to be fixed to a reasonable value that was consistent with the model. Thus, it is ideal for the evaluation of soil moisture memory as the additional source of predictability. In this paper we will refer to this ensemble as the climatological ensemble. It is important to note that while the soil moisture was fixed, the snow was evolving with time. We are therefore most interested in areas that are not snow covered or influenced by the history of snow cover.

The observed SSTs were taken from the ERA-40 dataset (Fiorino 2004), originally from Hadley Center and NCEP analyses using EOFs, cleaned up near the ice edges, and interpolated to daily values using a monthly mean conserving scheme for the ECMWF 40-year reanalysis. Anomaly correlations were taken with respect to the CRU near surface temperature analysis

without variance-adjustment (New et al, 2000). The observed precipitation shown in Figure 7 is from the CRU precipitation analysis.

In this paper we will look at the results for two-meter temperature since we are interested in a global field with an observational record. We found the effects on precipitation to be quite small and will therefore not show them here. This is consistent with previous work. Koster and Suarez (2002), Schlosser and Milly (2002), Kanamitsu et al. (2003) and Douville (2003) all found that soil moisture has a larger influence on near surface temperature than on precipitation.

The potential predictability (r) in this study is calculated according to Sardeshmukh et al (2000) as

$$r = \frac{\left(\frac{S}{N}\right)^2}{\sqrt{\left(\left(\frac{S}{N}\right)^2 + 1\right)\left(\left(\frac{S}{N}\right)^2 + \frac{1}{n}\right)}} \quad (\text{Eq. 1})$$

where S/N is the signal-to-noise ratio and n is the number of ensemble members. In this case the signal is the ensemble mean anomaly and the noise is the ensemble spread, which are defined as:

$$S = \left| \left(\frac{\sum_n T_n}{n} \right) - c \right| \quad (\text{Eq. 2})$$

$$N = \frac{\sum_n \left(T_n - \frac{\sum_n T_n}{n} \right)}{n}. \quad (\text{Eq. 3})$$

T_n is the temperature of an individual member, n is the number of members in the ensemble, and c is the temperature climatology from the respective ensemble for the years 1961-1990 (to match the climatology years used in the CRU data). In other words,

$$c = \frac{\sum_n \sum_t T_{nt}}{nt}, \quad (\text{Eq. 4})$$

where t is the number of years, and n is again the number of ensemble members. In the case of the climatological ensemble an estimate of the 1961-1990 climatology was calculated by

assuming a linear relationship in the difference between the climatologies of the two ensembles.

Both the signal and noise are averaged over time.

Potential predictability, as defined here, is the actual anomaly correlation that would occur in an infinite ensemble (with no sampling errors) of a perfect model (with no model errors) (Sardeshmukh et al 2000 and Compo and Sardeshmukh 2004). As shown in the appendix of Compo and Sardeshmukh (2004) this method of computing potential predictability is identical to the perfect model approach (assuming in turn that each member of the ensemble is truth), with the exception of sampling errors. It should be noted that, with the relatively small sample of 8 members and 12 years, errors in the estimates of signal and noise will occur. We have computed an estimate of the error in the noise by comparing the root mean square error of each ensemble mean versus observations to the ensemble spread (the noise as defined in equation 3). Error estimates were typically on the order of 30% for the regions considered in this study.

4. Regional Analysis of Soil Moisture Sensitivity

A primary focus of this paper is to better understand the ability of interactive soil moisture to improve real forecast skill of near-surface temperature, so we begin by looking at the differences in anomaly correlation against real observations between the interactive soil moisture ensemble and the climatological soil moisture ensemble. Figure 2 shows the anomaly correlation difference using CRU observed two-meter temperature. To focus on the points of interest the map has been masked by three criteria. First, the areas that are usually snow covered have been shaded gray. Of the areas without snow cover, the only areas that are color shaded are the areas where (1) the interactive soil moisture ensemble has an anomaly correlation greater than 0.3 and (2) the interactive soil moisture ensemble has a greater anomaly correlation than the climatological soil moisture ensemble. If either of these criteria is not met, the area is left white. The value of 0.3 is somewhat arbitrarily chosen, but skill below .3 is not considered very useful for seasonal forecasting. There are clearly many areas that are not shaded which suggests that

they are likely not sensitive to local soil moisture in this model. However there are some regions with a large sensitivity to soil moisture, and a survey of those regions will be the focus of this section.

In this paper we are only considering the *improvements* of anomaly correlation due to interactive soil moisture, and so we will refer to soil moisture sensitivity only in areas where the anomaly correlation has improved. It should be noted that the masked areas in Figure 2 include regions where the model anomaly correlation was harmed by interactive soil moisture. In fact, the decrease in anomaly correlation in the areas where there is a significant decrease with the interactive ensemble is only about 10% less than the average increase in anomaly correlation in the areas where there is a significant increase. In other words interactive soil moisture does only slightly more good than harm. We assume that many of the decreases in anomaly correlation are likely due to model error. The details of the exact causes of the decreases are beyond the scope of this paper. Also, it should be noted that by looking at the point-wise anomaly correlation, we are focusing on the local effects of soil moisture on temperature.

The areas that are sensitive to soil moisture include Northeastern Australia in January and February, the Sahara in March and April, Europe, Southeastern Africa, and Brazil in May and June, Western Australia, Northwestern Russia, Argentina and Western Canada in July and August, and Indo-China in September and October. In all the areas listed the difference in anomaly correlation in the majority of the region is significant at the 95% level based on a t-test (with the exception of Southeastern Africa, which will be discussed later). Other differences seen in figure 2 are either very small or not significant based on the t-test. All the above regions will be discussed in this section, with the exception of the Sahara, due to its extreme conditions. In addition to the regions listed above, there are two areas that do not appear to have soil moisture sensitivity while it would be expected from previous studies. Specifically, Yang et al (2004), Koster et al (2004) and others have seen sensitivity to soil moisture in the South-Central U.S., and Koster et al (2004), Thiaw and Mo (2005), and others have seen sensitivity to soil

moisture in the African Sahel. We will look at the South-Central United States in May and June and the Sahel in July and August in more detail in light of these studies.

Figures 3 through 7 show the regions in detail. Figure 3 shows the spatial average of the anomaly correlation for the interactive (vary) and climatological (fix) ensembles. Figure 4 shows the potential predictability averaged over the region. Figure 5 shows the soil moisture auto time-lag correlation for the interactive ensemble at one and two months lag. (The time-lag correlation for the climatological ensemble is undefined). A similar time-lag correlation was computed between soil moisture and evaporation, but the relative results were almost identical to the soil moisture auto correlation, so they are not shown here. Figure 6 shows the year-to-year soil moisture variability for each region, again for just the interactive ensemble since the climatological ensemble has no time-lag correlation. The soil moisture variability is defined as

$$\frac{\sum_n (sm - \overline{sm})^2}{n}, \quad (\text{Eq. 5})$$

where sm is the volumetric soil moisture fraction, \overline{sm} is the climatological volumetric soil moisture fraction, and n is the 53 years of the full interactive ensemble. Figure 7 shows the annual climatological cycle of precipitation for both the ECPC SFM and CRU observations.

4.1 Northeastern Australia (19S-25S, 135E-148E) in January/February

From the anomaly correlation map of Figure 2 it can be seen that Northeastern Australia shows sensitivity to soil moisture in January and February, which corresponds to the Australian monsoon season. The climatological annual precipitation cycle for this region is seen in the top panel of Figure 7. While the model overestimates the rainfall during the rainy season, the model correctly estimates the timing of the seasonal cycle, with peak precipitation in January and February. The area sensitive to soil moisture is small here, however the increase in anomaly correlation is large (Figure 3). The sensitivity to soil moisture is greater during El Nino/

Southern Oscillation (ENSO) years and covers a greater area in those years. (The anomaly correlation with the interactive ensemble is 0.92, while the correlation with the climatological ensemble is 0.61 based on the 3 ENSO years included in this study). Timbal et al (2002) found that soil moisture was a key link between the Southern Oscillation Index and the Australian monsoon. It is therefore not surprising that there is an increased anomaly correlation during ENSO years with interactive soil moisture.

In addition to finding locations and times with soil moisture sensitivity, it is also a goal of this study to look for potential sources of the sensitivity. To that aim we look at the soil moisture time-lag correlation and year-to-year variability. While the soil moisture time-lag correlation for Northeastern Australia is fairly unremarkable (Figure 5), the year-to-year variability in soil moisture shown in Figure 6 is quite remarkable. Large values of soil moisture variability do not guarantee an increase in predictability, but they do suggest a difference in predictability should be expected. The soil moisture variability is likely due to the location of this January and February sensitivity, which is on the southern border of the Australian monsoon where the soil moisture is dependent on the exact location of the southern extent of the monsoon rainfall. In addition to the large variability, the soil here is neither extremely wet nor extremely dry (compare the Northeastern Australian value of 0.25 to the global average of 0.28). Koster et al (2004) suggested that mid-values of soil moisture (or semi-arid regions) encourage soil moisture sensitivity.

As seen in Figure 4, there is not a corresponding increase in the theoretical measure of potential predictability in January and February with interactive soil moisture. This discrepancy will be discussed in section 5.

4.2 Southeastern Africa (18S-26S, 26E-36E) in May/June, Western Australia (15S-35S, 115E-135E) in July/August, and Argentina (40S-25S, 70W-55W) in July/August

Southeastern Africa (essentially Mozambique and Zimbabwe) has an interesting area of increase in anomaly correlation due to interactive soil moisture that appears in May and June (Figure 2). This is shortly after the end of the rainy season in that region. The top panel of Figure 7 shows that, as in Australia, the model overestimates the observed rainfall, but reproduces the annual cycle. This area of Africa is particularly interesting due to the likely relationship between the winds and the surface temperature. A simple correlation between the surface temperature over Southeastern Africa and the 925mb meridional winds over the Mozambique Channel (between the African continent and Madagascar) of 0.65 (based on 57 years of NCEP reanalysis data) suggests that the near surface temperature drives the winds in the Mozambique Channel and may influence the Somali jet, which provides moisture into the monsoonal Indian subcontinent. A year-by-year visual analysis of the 12 years in this study suggested that anomalous cold temperatures associated with wet soil strengthen the northward flow in the channel, while warmer temperatures associated with dry soil weaken the flow. More study is necessary to precisely determine this relationship; however, it seems the sensitivity to soil moisture here is also seen in the winds.

The soil moisture sensitivity in Southeastern Africa can be attributed in part to soil moisture memory (Figure 5). In May and June (after the end of the rainy season) the interactive soil moisture ensemble still retains information about the previous rainy season, which could produce a larger, more accurate signal. The one-month soil moisture time-lag correlation between May and June and the previous month is extremely high at 0.96. This suggests that the climatological ensemble (which has no soil moisture memory) will not be able to have the same skill. In addition the soil moisture variability in this area is larger than average (Figure 6), which is likely an additional source of soil moisture sensitivity. It is surprising, given the high values of soil moisture time-lag correlation and variability, that the increase in anomaly correlation with interactive soil moisture in this region is quite small. We suspect that a longer time record would

show a larger increase. There is not a corresponding increase in potential predictability due to interactive soil moisture in Southeastern Africa.

As mentioned earlier, the difference in anomaly correlation is generally not significant in Southeastern Africa. Only a small part of this region has a difference that is significant at the 95% level. This allows for the possibility that the sensitivity in this area might not be robust. However the soil moisture memory and variability suggest that it is robust, and given the potential remote effects of the region, it was determined to include Southeastern Africa in the survey of regions to encourage further study.

We look now at Western Australia, which is similar to Southeastern Africa in the potential sources of soil moisture sensitivity. Western Australia, which is largely desert, has a rain maximum around February coming from the Australian monsoon to the north, and more rain coming from the southwest in the following months. This region receives almost no rainfall between July and November (Figure 7). It is in July and August, after the rainfall, that the near-surface temperature is sensitive to soil moisture. Since the rainfall between December and June is quite variable for a desert region, soil moisture memory is essential for a reasonable forecast in the dry months. Like Southeastern Africa, not only does the soil moisture sensitivity occur after the rainy season, but the soil moisture time-lag correlation also suggests soil moisture memory is important here, with both one and two month correlations over 0.9 (Figure 5). However, while there is an increase in anomaly correlation, there is a decrease in potential predictability with the interactive soil moisture ensemble.

Argentina (the Pampas region) is not as dry as Western Australia, but is still relatively dry with a seasonal cycle in precipitation (Figure 7). Like Southeastern Africa and Western Australia the sensitivity to soil moisture occurs after the wet season. Also similar is the fairly high soil moisture time-lag correlation, suggesting again that soil moisture plays a key role in determining near-surface temperature after the rainy season.

Another commonality between Western Australia and Argentina is that they are the two regions in this study that were found to significantly overestimate noise (or underestimate potential predictability). This result is based on a comparison between ensemble spread and the root-mean-square-error between the ensemble and observations. For these two regions the ensemble spread was close to 40% higher than the RMSE error.

4.3 Indo-China (10N-24N, 96E-110E) in September/October, and Northern Brazil (10S-Eq, 75W-50W) in May/June

Another area where the difference in anomaly correlation points to soil moisture sensitivity is Indo-China in September and October (Figures 2 and 3), which is at the end of the monsoon season (third panel of Figure 7). This timing, with the sensitivity to soil moisture occurring after the peak in rainfall, is similar to the regions discussed in section 4.2. Also like other regions, the model overestimates the rainfall here compared to observations, but correctly represents the seasonal cycle. There is little year-to-year variability in soil moisture here (Figure 6), and surprisingly little soil moisture time-lag correlation (Figure 5). It is possible that soil moisture memory is important for the near-surface temperature anomaly correlation on shorter time scales, but that cannot be determined in this study. It is worthy to note that the anomaly correlation for the three ENSO years covered in this study is very high (almost 0.9) for the interactive soil moisture ensemble and low (about 0.2) for the climatological ensemble. It has been shown (Singhrattna et al 2005) that since 1980 the monsoon rainfall in Thailand is highly correlated to ENSO. Since soil moisture is essential for predicting temperature during ENSO years, it is reasonable to suggest that soil moisture might also be key in predicting precipitation, although further study is necessary to determine this relationship.

Northern Brazil is similar to Indo-China in that the soil moisture sensitivity occurs at the end of the rainy season and both have large seasonal precipitation cycles. Neither region has large soil moisture variability, with extremely small values in Brazil. And, neither region

exhibits long-term soil moisture memory. Again it is possible that shorter-term soil moisture memory plays a role in the soil moisture sensitivity. This idea is supported by the fact that in considering June alone, both the difference in anomaly correlation between the two ensembles and especially the time-lag correlation increase compared to the two-month (May/June) values.

4.4 Europe (40N-50N, 0-20E) in May/June, Northwestern Russia (60N-70N, 45E-85E) in July/August, and Western Canada (48N-53N, 122W-105W) in July/August

As seen in Figures 2 and 3, three northern latitude locations have an increase in anomaly correlation with interactive soil moisture: Europe, Northwestern Russia, and Western Canada. The bottom panel of Figure 7 shows that none of the regions have a strong annual precipitation cycle. In addition none of the regions have outstanding values of soil moisture time-lag correlations (Figure 5). Consequently, the sources of the soil moisture sensitivity appear more indirect than for other lower-latitude regions considered in this study.

Looking at year-to-year soil moisture variability (Figure 6), neither Russia nor Canada shows much variability, but in Europe there is reasonably large variability, which could explain some of the sensitivity there. It is also worthy to note that in Russia there is a corresponding increase in potential predictability with interactive soil moisture in this region (Figure 4), while both Europe and Canada show a slight decrease.

While these regions are not an exhaustive list of areas with soil moisture sensitivity, they are some of the largest (either in area or magnitude of change) and most interesting areas found in the ECPC SFM. Other areas with sensitivity could likely be found if remote responses were considered. It must also be said that even though there are limited areas and times with sensitivity to soil moisture, the increase in skill in these areas alone justifies the need for evolving soil moisture for a global seasonal forecast.

4.5 South-Central U.S. (30N-37N, 103W-84W in May/June), and the Sahel (10N-20N, 342E-18W) in July/August

As mentioned earlier, there are two regions we will consider that did not show an increase in anomaly correlation with interactive soil moisture. While the South-Central U.S. has been documented as having sensitivity to soil moisture in the summer, there is no increase in anomaly correlation for the South-Central U.S. with the ECPC SFM (Figure 3). The ECPC SFM does, however, produce an area of increase in potential predictability in May and June for that area (Figure 4). This significant increase (based on a t-test at the 95% level) occurs where the difference in noise (Eq 3) is large while the difference in signal (Eq 2) is even larger, with the interactive ensemble having both a larger signal and more noise than the climatological ensemble. More will be said about this later. The disagreement between the two measures of predictability suggests that while the interactive soil moisture produces a large signal in temperature (resulting in an increase in potential predictability), the signal is not correct in this model, or cannot be predicted by knowing SSTs and varying soil moisture. The precipitation for this region is shown in the second panel of Figure 7. While the differences between the model and observed precipitation are not large, based on Yang et al (2004), it seems likely that a more accurate rainfall would improve the signal.

In the African Sahel neither anomaly correlation nor potential predictability shows significant sensitivity to soil moisture (not shown). This is surprising since, as mentioned earlier, the Sahel has been shown in other studies to be an area sensitive to soil moisture in the summer. In fact, a study using the same model for a 50-year period finds large sensitivity to the land surface processes in that area (DeHaan et al, 2006). Since the 12-year record of the current study only includes drought years in the Sahel, it is not surprising that there is little year-to-year variability in that time. In fact in the Sahel the year-to-year soil moisture variability for the 50-year record is 40% larger than the global average, while the variability for the 12-year record used here is 25% less than the global average. It is therefore likely that the lack of sensitivity in

the Sahel is due to the short time record of this study and the relative lack of variability during the years chosen.

5. Potential Predictability and Anomaly Correlation

As we consider the potential predictability and anomaly correlation from the regions discussed in section 4, there are two issues that need to be addressed concerning the relationship between the two measures of skill. First we will look at the interactive ensemble alone to compare potential predictability and anomaly correlation for the regions discussed in the last section. Secondly, the discrepancies that arise when comparing the two ensembles and their respective anomaly correlations and potential predictabilities will be discussed.

5.1 Interactive Ensemble

Figure 8 is one look at the relationship between anomaly correlation and potential predictability for the interactive ensemble. On the x-axis is the signal-to-noise ratio and on the y-axis is anomaly correlation. The solid line is the potential predictability for an eight-member ensemble according to Equation 1. To look globally at the relationship we computed the signal-to-noise ratio and the anomaly correlation for $10^{\circ} \times 10^{\circ}$ boxes for all land areas without snow. We then binned all the points with signal-to-noise ratio less than 0.5, between 0.5 and 1.0, between 1.0 and 1.5, and greater than 1.5. The result is given by the pink boxes. As discussed in Compo and Sardeshmukh (2004) and Sardeshmukh et al (2000), the fact that boxes clearly fall well below the potential predictability indicates systematic model error, which is not surprising. More importantly for this study are the circles, which represent the same calculation for each region of improved anomaly correlation discussed in this study. It is clear that these regions are exceptional in how close the anomaly correlation is to the potential predictability. In other words, in these regions the model performs as well as could be expected, and there is relatively little systematic model error. It is of some concern that four of the points lie above the potential

predictability line. However, Argentina and Western Australia are the two regions in which it appears that the noise has been overestimated. Southeastern Africa and Europe are likely above the line due to other sampling errors.

5.2 Differences between the Interactive Ensemble and the Climatological Ensemble

We now switch to considering the differences between the two ensembles for both measures of skill. In the regions discussed in section 4, only Northwestern Russia and, to some degree, Argentina showed agreement between anomaly correlation and potential predictability. In those cases both measures of predictability increased with the use of interactive soil moisture. Northeastern Australia, Southeastern Africa, Europe, Northern Brazil, Western Canada and Indo-China all showed similar values of potential predictability between the two ensembles while there was an increase in anomaly correlation with the interactive ensemble. Finally, in the South-Central U.S. and Western Australia anomaly correlation and potential predictability gave opposite results. The lack of agreement between these two measures of model skill is cause for concern, so we look here at the relationship in more detail.

We begin by considering the global, long-term relationship between anomaly correlation and potential predictability. The correlation for the 49-year AMIP run between potential predictability and anomaly correlation is approximately 0.7 over land, suggesting that there is a clear relationship between real and theoretical skill. A similar correlation for the 12 years used in this study is over 0.5. This indicates that a longer time record would improve the relationship, but there is still a reasonable correlation between the two measures of skill. However, when we look at the *differences* in skill between the interactive and climatological ensembles the relationship becomes much less clear. The correlation between the *difference* in anomaly correlation and the *difference* in potential predictability is just over 0.1.

To further understand the differences in potential predictability between the two sets of runs, the signal and noise have been considered separately, since potential predictability is

similar to the signal-to-noise ratio. Comparing the globally and seasonally averaged signal between the ensembles shows that the interactive ensemble has a signal of about 10% more than the climatological ensemble, while comparing the noise between the two ensembles shows that the interactive ensemble has approximately 30% more noise than the climatological ensemble. The greater signal for the interactive ensemble is a favorable result for the interactive soil moisture runs. The greater difference in noise is not surprising, however, considering that the soil moisture is the same for all eight members of the climatological ensemble, which reduces the spread between the members. As a result of the small increase in signal but a greater increase in noise, the globally and seasonally averaged potential predictability of the interactive ensemble is less than that of the climatological ensemble. The less noise in climatological ensemble, which is the result of the unrealistic assumption of non-interactive soil moisture, mutes the effect of the signal due to evolving soil moisture in the interactive ensemble.

The muting of the effect of the signal can be seen by looking at the spatial correlation between the signal and potential predictability and the correlation between the noise and potential predictability. The full fields (not the differences) of the signal and potential predictability have a correlation of approximately 0.1, while the noise and potential predictability have a correlation of approximately -0.6. (These values are global and seasonal averages over both ensembles). *This implies that the noise plays a larger part than the signal in determining spatial pattern of potential predictability.* However when considering the difference in signal, difference in noise, and difference in potential predictability (between the two ensembles), we find that the spatial correlation between the difference in signal and the difference in potential predictability is approximately 0.4, while the correlation between the difference in noise and the difference in potential predictability is approximately -0.1. *This indicates that the difference in potential predictability is primarily driven by the difference in signal, and the influence of the noise becomes secondary.*

Since the difference in potential predictability is driven by the difference in signal, rather than the difference in noise, and since potential predictability of the interactive ensemble is generally less than the climatological predictability, it is not surprising that a greater value of potential predictability for one ensemble over the other does not necessarily correspond to a greater value of model skill (anomaly correlation) for the same ensemble. In the cases where the potential predictability values from the two ensembles are quite close, it is reasonable to guess that without the relative increase in noise, the interactive ensemble would have a higher potential predictability value. Western Australia has the largest discrepancy between the two measures of skill. Here the difference in potential predictability could be overly influenced by a small signal, and again the potential predictability for the interactive ensemble might be higher without the change in noise. The case of the South-Central U.S. is a little different. While the difference in potential predictability could again be too dependent on the signal, model error is likely to blame for the poor anomaly correlation. While we can attempt to “explain” the inconsistencies between anomaly correlation and potential predictability in this manner, it is clear that if anomaly correlation was not considered a very different outcome would result from looking at the difference in potential predictability alone.

It could be argued that the lack of agreement between anomaly correlation and potential predictability is simply due to our experimental set-up (use of climatological soil moisture). However, it also points to a problem that could be seen when doing a comparison between any two model runs. Unless the relative values of signal and noise are similar, inconsistencies will arise which can artificially increase the importance of either signal or noise. So, while potential predictability can be a useful tool in considering the strengths and weaknesses of a single model (as in Figure 8), it needs to be used with caution when comparing two sets of model runs. In other words, a larger value of potential predictability for one ensemble compared to the other does not necessarily imply that the model skill is greater for that ensemble, and therefore, the comparison has limited use in evaluating differences in model physics.

6. Conclusions

In this study we have looked at two sets of 12-year 8-member integrations from the ECPC Seasonal Forecast Model forced by observed SSTs. One set had a fully integrated land surface model with evolving soil moisture, while the other had soil moisture fixed to the seasonally varying climatological value so that it did not respond to the atmospheric component of the model. This experiment was designed to understand how much and where the predictability (due to observed SST) is increased by including the soil moisture component into the forecast system. The differences between these two sets of runs were examined using two different measurements of predictability: anomaly correlation with observations and potential predictability.

In the first part of the paper, we look at nine regions which all showed an increase in anomaly correlation due to interactive soil moisture at different times during the year. For each of these regions three fields were considered, in addition to the skill measures, to help better understand the causes of the soil moisture sensitivity: soil moisture time-lag correlation, soil moisture variability, and the annual precipitation cycle. We found four basic divisions among potential sources of soil moisture sensitivity. (1) Northern Australia is unique in the regions studied due to its extremely high year-to-year variability of soil moisture. (2) Southeastern Africa, Western Australia, and Argentina are similar to each other in that all three areas are sensitive to soil moisture in the months following the peak rainy season, and all three have high soil moisture memory. (3) Brazil and Indo-China are similar to the three previous areas in that they both show soil moisture sensitivity in the months following the rainy season. However, these two regions, surprisingly, have low soil moisture memory. It is possible that the soil moisture memory on a shorter time scale is larger. (4) Finally Europe, Western Canada and Northwestern Russia all behave similarly, with no strong seasonal cycle in precipitation and no clear reason for the soil moisture sensitivity.

Some non-linear and non-local soil moisture sensitivities were also seen in a few of the regions. In Northern Australia and Indo-China sensitivity to soil moisture greatly increased during ENSO years. In Southeastern Africa it is possible that the effects of soil moisture go beyond local near surface temperature and could be seen remotely in the winds as well.

There were two regions considered that did not show an increase in anomaly correlation with interactive soil moisture for the ECPC SFM. Both the South-Central U.S. and the African Sahel are areas where soil moisture sensitivity is expected from other studies. It was found that the South-Central U.S. had an increased signal with interactive soil moisture, but an improved rainfall prediction was likely necessary for an improved anomaly correlation. For the Sahel, it was determined that the years chosen in this study did not vary enough to see the sensitivity to soil moisture.

The second part of this paper focused on the relationship between anomaly correlation and potential predictability. It was found that in the nine regions where anomaly correlation was improved with interactive soil moisture, the anomaly correlation and potential predictability were close in value when considering the interactive ensemble alone. This suggests that the model predicts near-surface temperature as well as could be expected in those regions.

When considering both ensembles, there were many discrepancies between differences in sensitivities to soil moisture found with anomaly correlation compared to those found using potential predictability. Those discrepancies are partly due to the short time record of this study, but are also largely due to a difference in noise and signal between the two ensembles. The potential predictability is primarily a ratio between signal and noise, and both signal and noise change independently with our current experimental setup. Particularly, the use of climatological soil moisture reduces the noise unrealistically for that ensemble due to the use of the same seasonally varying soil moisture every year and for each member. The relative increase in noise with the interactive ensemble overwhelms the increase in signal found in the interactive ensemble, and makes the comparison of potential predictability between the two ensembles

inconsistent. Because of this, the increase in potential predictability of one experiment over another cannot generally be used to estimate the increase in true skill.

Acknowledgements

The authors wish to thank Tosiya Nakaegawa for assistance in creating the integrations, Sarah Lu for implementing the Noah LSM, and John Roads, Gil Compo and David De Haan for helpful suggestions regarding this work. The helpful comments of three anonymous reviewers are also gratefully acknowledged. This study was supported by NOAA NA17RJ1231. The views expressed herein are those of the authors and do not necessarily reflect the views of NOAA. Figures 1 and 2 were created with GrADS software.

References

- Alpert, J.C., M. Kanamitsu, P.M. Caplan, J.G. Sela, G.H. White, and E. Kalnay, 1988: Mountain induced gravity wave drag parameterization in the NMC medium-range model. Preprints of the Eighth Conference on Numerical Weather Prediction, Baltimore, MD, American Meteorological Society, 726-733.
- Chou, M. -D. and M. J. Suarez, 1994: An efficient thermal infrared radiation parameterization for use in General Circulation Models. Technical Report Series on Global Modeling and Data Assimilation, National Aeronautical and Space Administration/TM-1994-104606, 3, 85 pp.
- , and K. -T. Lee, 1996: Parameterizations for the absorption of solar radiation by water vapor and ozone. *J. Atmos. Sci.*, **53**, 1203-1208.
- Compo, G. P. and P.D. Sardeshmukh, 2004: Storm Track Predictability on Seasonal and Decadal Scales. *J. Climate*, **17**, 3701-3720.
- DeHaan, L.L., M. Kanamitsu, C. -H. Lu, and J.O. Roads, 2006: A Comparison of the Noah and OSU Land Surface Models in the ECPC Seasonal Forecast Model. Submitted to *J. Hydrometeor.*
- Dirmeyer, P.A., 2000: Using a Global Soil Wetness Dataset to Improve Seasonal Climate Simulation. *J. Climate*, **13**, 2900-2922.
- Douville, H., 2003: Assessing the Influence of Soil Moisture on Seasonal Climate Variability with ACGMs. *J. Hydrometeor.*, **4**, 1044-1066.
- Ek, M.B., K.E. Mitchell, Y. Lin, E. Rogers, P. Grunmann, V. Koren, G. Gayno, and J.D. Tarpley, 2003: Implementation of Noah land surface model advances in the National Centers for Environmental Prediction operational mesoscale Eta model. *J. Geophys. Res.*, **108**, 8851-8866.
- Fennessy, M.J., and J. Shukla, 1999: Impact of initial soil wetness on seasonal atmospheric prediction. *J. Climate*, **12**, 3167-3180.
- Fiorino, M., 2004: A Multi-decadal Daily Sea Surface Temperature and Sea Ice Concentration Data Set for the ERA-40 Reanalysis. ERA-40 project Report Series. ECMWF, Shinfield Park, Reading, RG2 9AX, UK. 16pp.

- Kanae, S., Y. Hirabayashi, T. Yamada, and T. Oki, 2006: Influence of “Realistic” Land Surface Wetness on Predictability of Seasonal Precipitation in Boreal Summer. *J. Climate*, **19**, 1450-1460.
- Kanamitsu, M., A. Kumar, H. -M. H. Juang, W. Wang, F. Yang, J. Schemm, S. -Y. Hong, P. Peng, W. Chen and M. Ji, 2002: NCEP Dynamical Seasonal Forecast System 2000. *Bull. Amer. Met. Soc.*, **83**, 1019-1037.
- , C. -H. Lu, J. Schemm and W. Ebisuzaki, 2003: The predictability of soil moisture and near surface temperature in hindcasts of NCEP Seasonal Forecast Model. *J. Climate*, **16**, 510-521.
- Koster, R.D., P.A. Dirmeyer, A.N. Hahmann, R. Ijpelaar, L. Tyahla, P. Cox, and M.J. Suarez, 2002: Comparing the Degree of Land-Atmosphere Interaction in Four Atmospheric General Circulation Models. *J. Hydrometeor.*, **3**, 363-375.
- and M.J. Saurez, 2003: Impact of Land Surface Initialization on Seasonal Precipitation and Temperature Prediction. *J. Hydrometeor.*, **4**, 408-423.
- , P.A. Dirmeyer, Z. Guo, G. Bonan, E. Chan, P. Cox, C.T. Gordon, S. Kanae, E. Kowalczyk, D. Lawrence, P. Liu, C. -H. Lu, S. Malyshev, B. McAvaney, K. Mitchell, D. Mocko, T. Oki, K. Oleson, A. Pitman, Y.C. Sud, C.M. Taylor, D. Verseghy, R. Vasic, Y. Xue, and T. Yamada, 2004: Regions of Strong Coupling Between Soil Moisture and Precipitation. *Science*, **305**, 1138-1140.
- New, M., M. Hulme, and P. Jones, 2000: Representing twentieth-century space-time climate variability. Part II: Development of 1901-96 monthly grids of terrestrial surface climate Source. *J. Climate*, **13**, 2217 –2238.
- Oglesby, R.J., S. Marshall, D.J. Erickson III, J.O. Roads, and F.R. Robertson, 2002: Thresholds in atmosphere-soil moisture interactions: Results from climate model studies. *J. Geophys. Res.*, **107**, 4224-4339.
- Sardeshmukh, P.D., G.P. Compo, and C. Penland, 2000: Changes of Probability Associated with El Niño. *J. Climate*, **13**, 4268-4286.

- Schlosser, C.A. and P.C.D. Milly, 2002: A Model-Based Investigation of Soil Moisture Predictability and Associated Climate Predictability. *J. Hydrometeor.*, **3**, 483-501.
- Singhrratna N., B. Rajagopalan, K. Kumar, and M. Clark, 2005: Interannual and interdecadal variability of Thailand summer monsoon season. *J. Climate*, **18**, 1697-1708.
- Simmonds, I. and P. Hope, 1998: Seasonal and Regional Responses to Changes in Australian Soil Moisture Conditions. *Int. J. Climatol.*, **10**, 1105-1139.
- Slingo, J.M., 1987: The development and verification of a cloud prediction model for the ECMWF model. *Quart. J. Roy. Meteor. Soc.*, **113**, 899-927.
- Thiaw, W.M. and K.C. Mo, 2005: Impact of Sea Surface Temperature and Soil Moisture on Seasonal Rainfall Prediction over the Sahel. *J. Climate*, **18**, 5330-5343.
- Tiedtke, M., 1983: The sensitivity of the time-mean large-scale flow to cumulus convection in the ECMWF model. Proceedings of the ECMWF Workshop on Convection in Large-Scale Models, 28 November-1 December 1983, European Centre for Medium-Range Weather Forecasts, Reading, England, 297-316.
- Timbal, B., S. Power, R. Colman, J. Viviand, and S. Lirola, 2002: Does Soil Moisture Influence Climate Variability and Predictability over Australia? *J. Climate*, **15**, 1230-1238.
- Tippett M.K., 2006: Filtering of GCM simulated Sahel precipitation. *Geophys. Res. Lett.*, **33**, L01804.
- Yang, F., A. Kumar, and K.M. Lau, 2004: Potential Predictability of U.S. Summer Climate with “Perfect” Soil Moisture. *J. Hydrometeor.*, **5**, 883-895.
- Zhang, H., and C.S. Frederiksen, 2003: Local and Nonlocal Impacts of Soil Moisture Initialization on AGCM Seasonal Forecasts: A Model Sensitivity Study. *J. Climate*, **16**, 2117-2137.

Figure captions

Fig. 1. JJA 2m T anomaly correlation with CRU data from the 50-year, 12-member AMIP simulation of the ECPC SFM.

Fig. 2. Difference in anomaly correlation of 2m T between the interactive ensemble and the climatological ensemble. Masking is described in the text.

Fig. 3. 2m T anomaly correlations for the interactive (vary) and climatological (fix) ensembles averaged over the regions of interest. The average of each anomaly correlation is for the season discussed in the text.

Fig. 4. Same as Figure 3, but for potential predictability.

Fig. 5. 1 and 2 month soil moisture time-lag correlations for the interactive ensemble averaged over the regions of interest. Each correlation is for the season discussed in the text.

Fig. 6. Year-to-year soil moisture variability (in units of $1000 \cdot (\text{volumetric soil moisture})^2$) for the interactive ensemble averaged over the regions of interest. Each average is for the season discussed in the text. The global value is the annual average.

Fig. 7. The climatological (1961-1990) annual cycle of precipitation for both the ECPC SFM (GSM) and CRU observations (Obs) in $\text{kg/m}^2/\text{day}$.

Fig. 8. Anomaly correlation (y-axis) plotted against the signal-to-noise ratio (x-axis). The solid line is the theoretical relationship between the two (potential predictability), the pink squares

show the binned global average with error bars, and the colored circles show the regions discussed in the text.

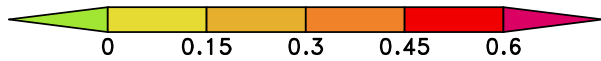
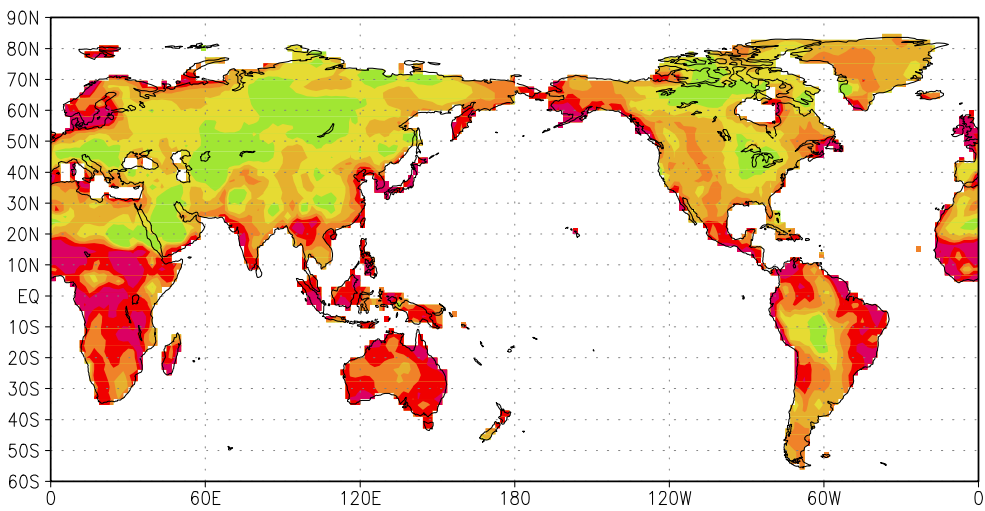


Fig 1: JJA 2mT anomaly correlation with CRU data from the 50-year, 12-member AMIP simulation of the ECPC SFM

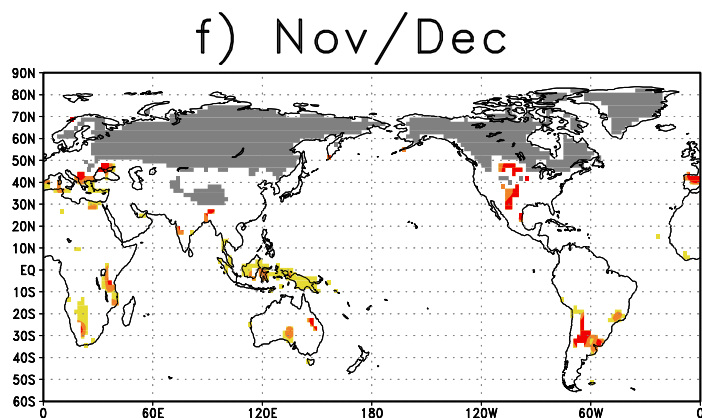
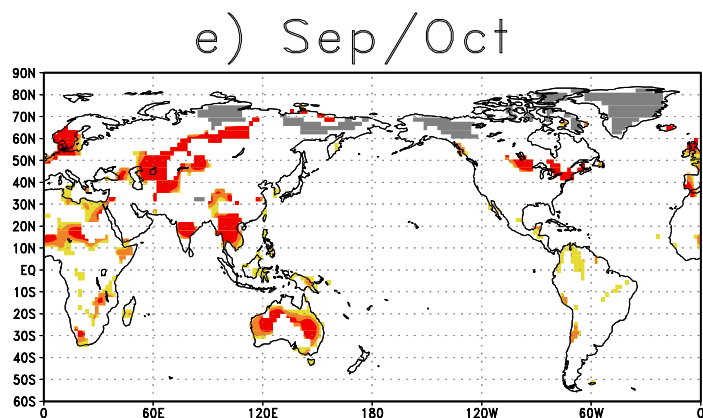
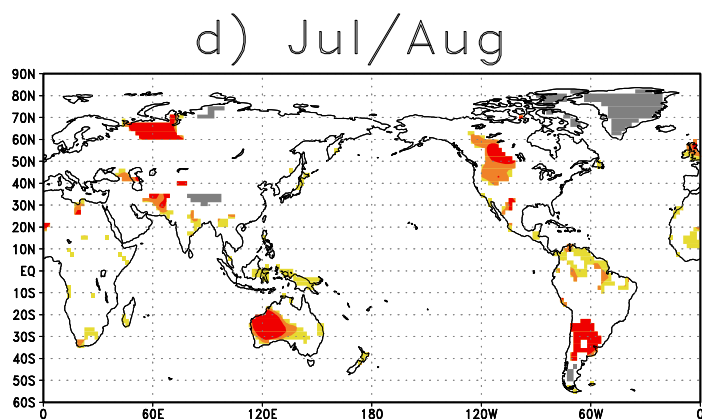
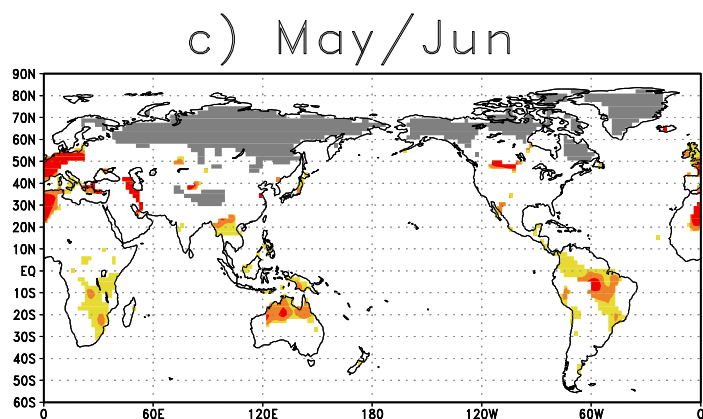
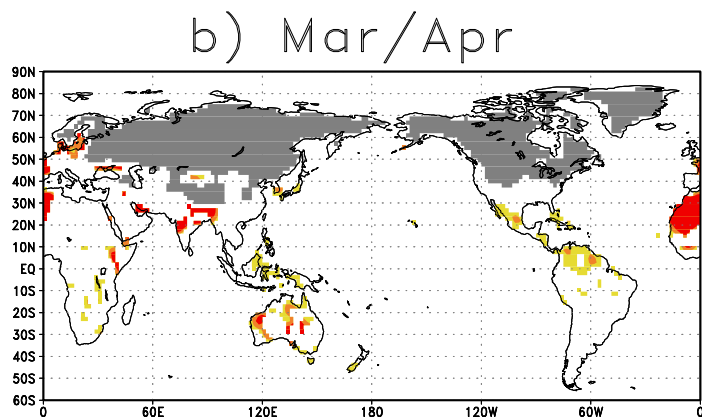
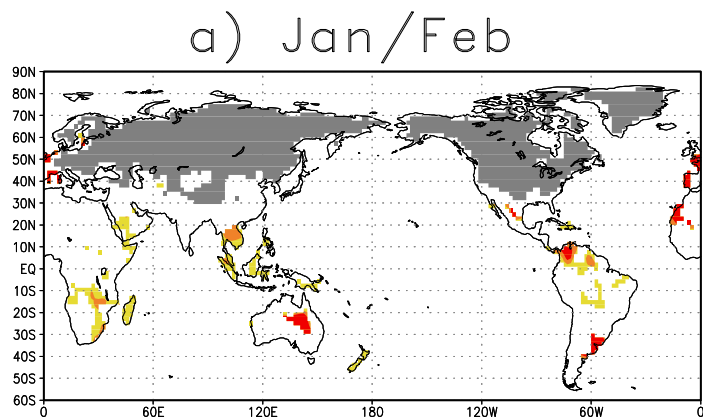


Fig. 2 Difference in 2m T anomaly correlation between interactive and climatological ensembles. Shading explained in text.

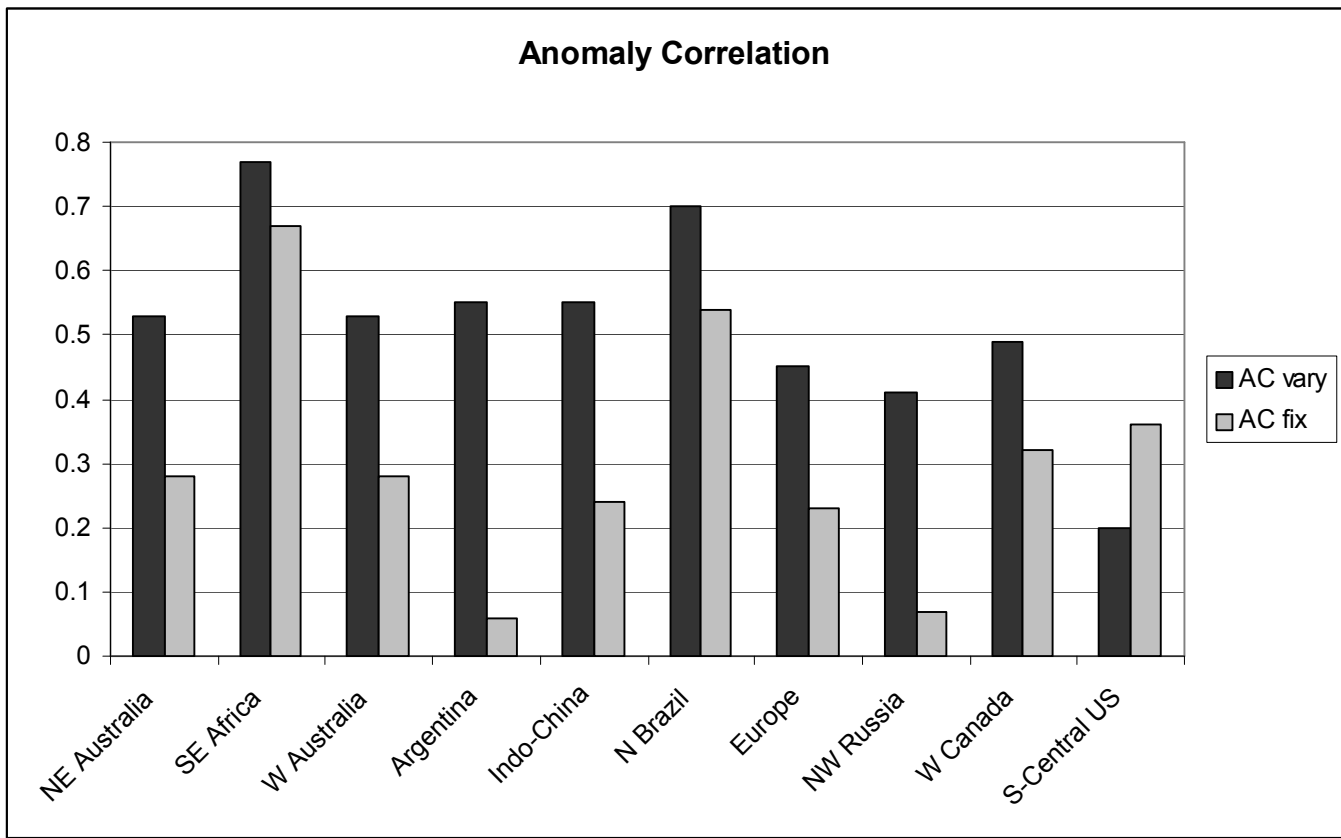


Figure 3: 2m T anomaly correlations for the interactive (vary) and climatological (fix) ensembles averaged over the regions of interest. The average of each anomaly correlation is for the season discussed in the text.

Potential Predictability

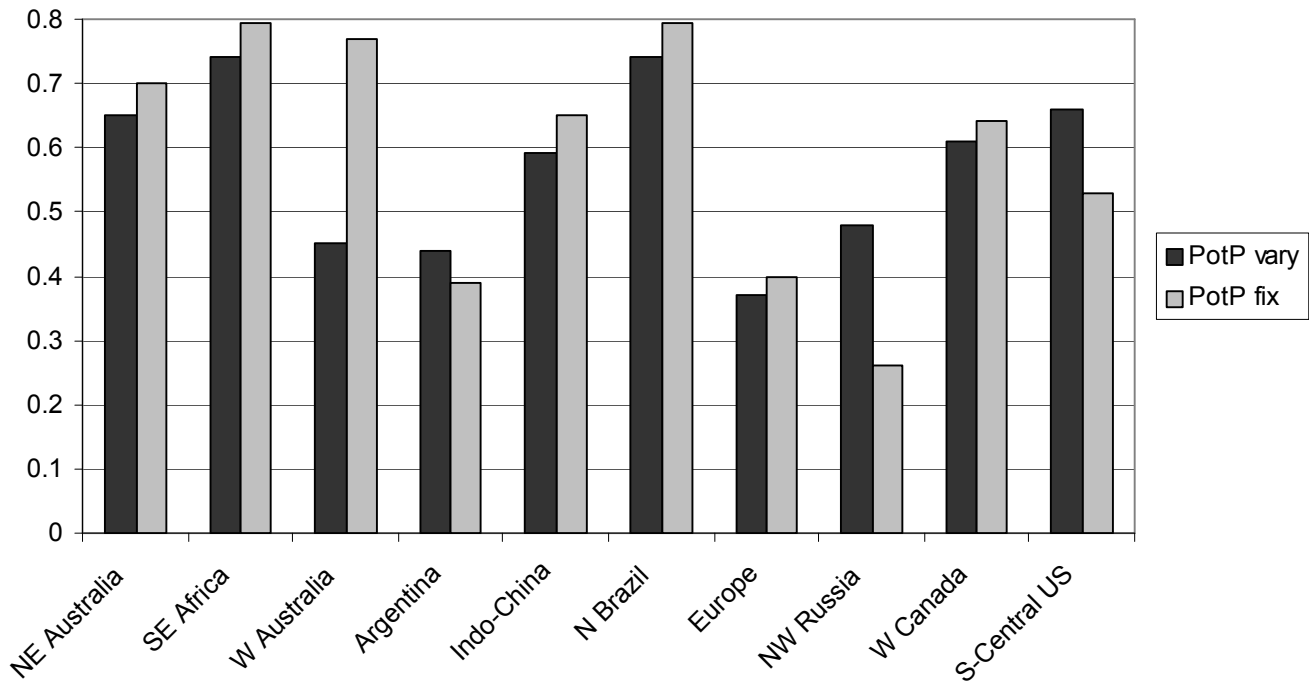


Figure 4: Same as for Figure 3, but for potential predictability.

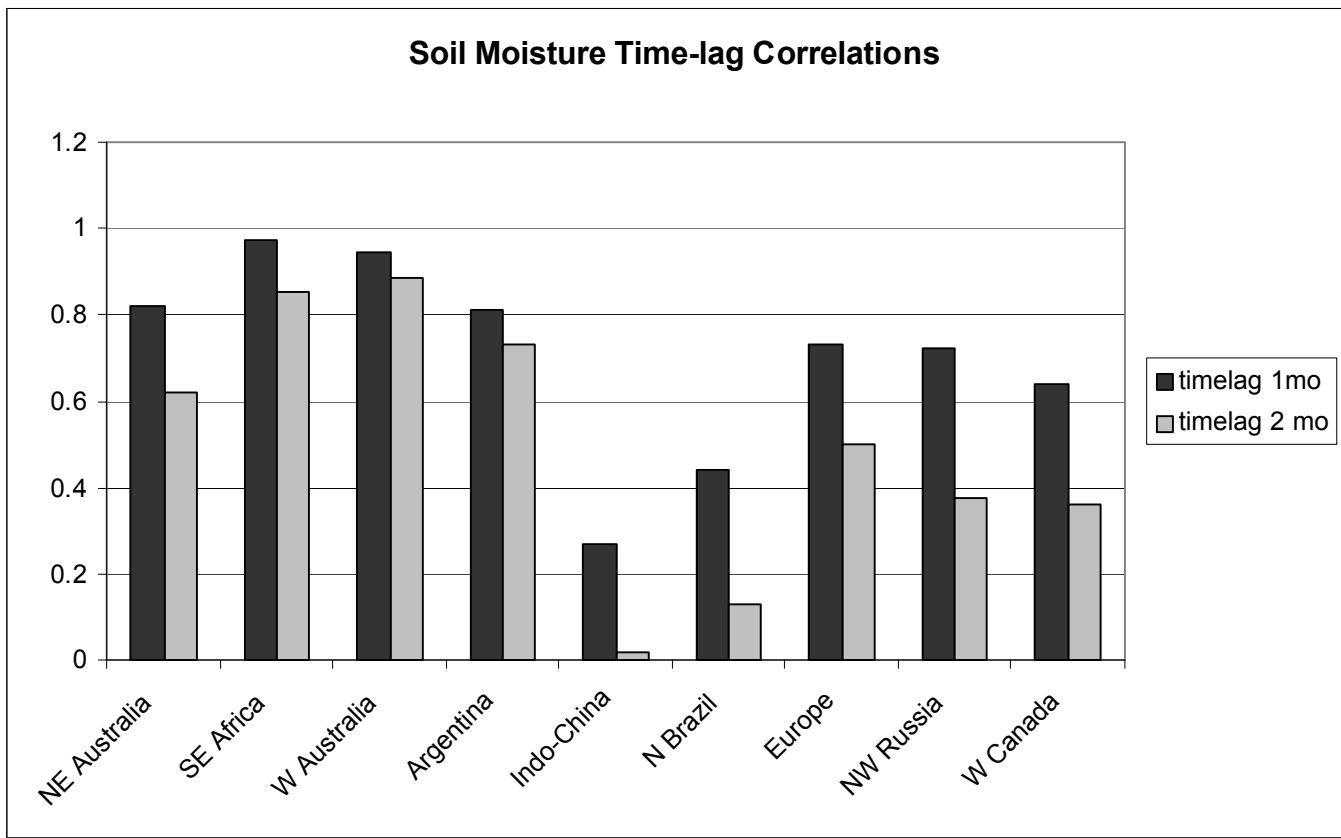


Figure 5: 1 and 2 month soil moisture time-lag auto-correlations for the interactive ensemble averaged over the regions of interest.

Soil Moisture Variability

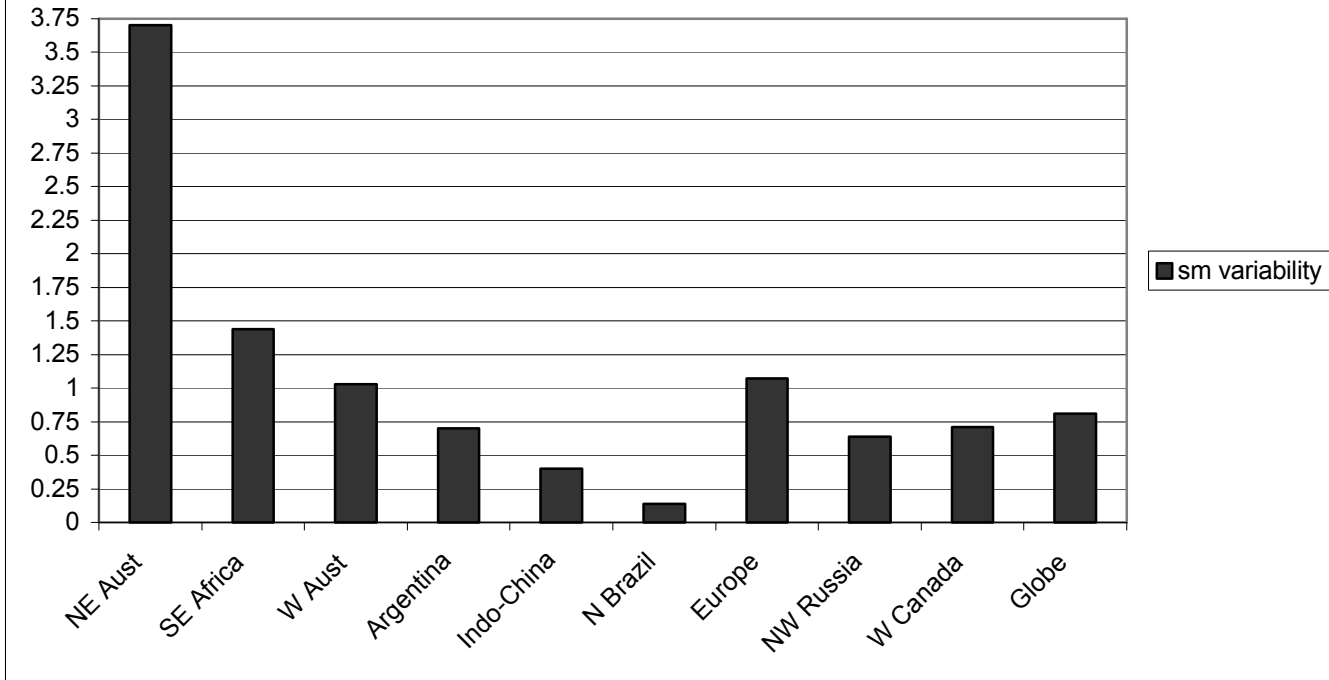


Figure 6: Year-to-year soil moisture variability (in units of $1000 \times (\text{volumetric soil moisture})^2$) for the interactive ensemble averaged over the regions of interest. Each average is for the season discussed in the text. The global value is the annual average.

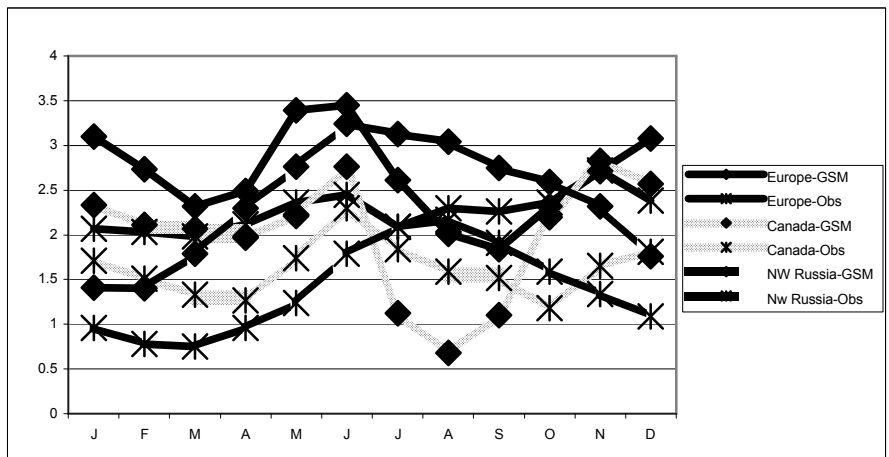
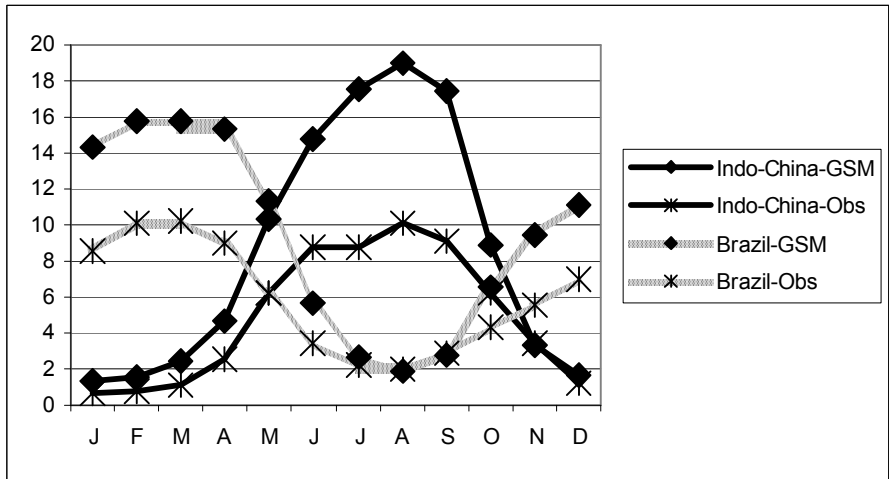
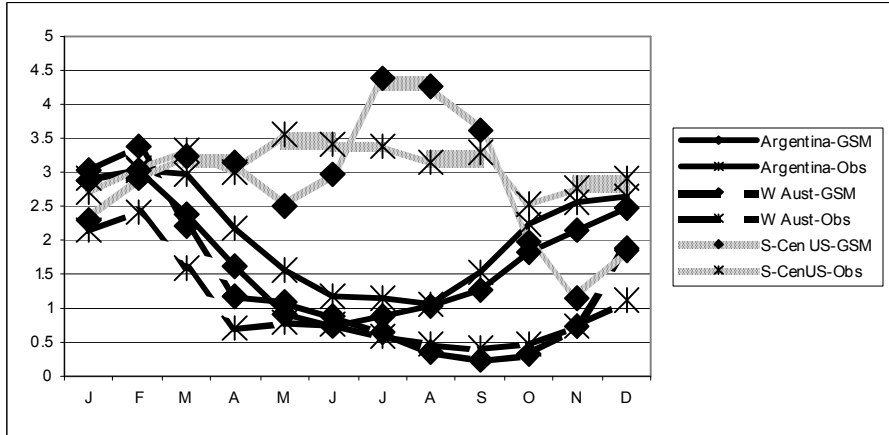
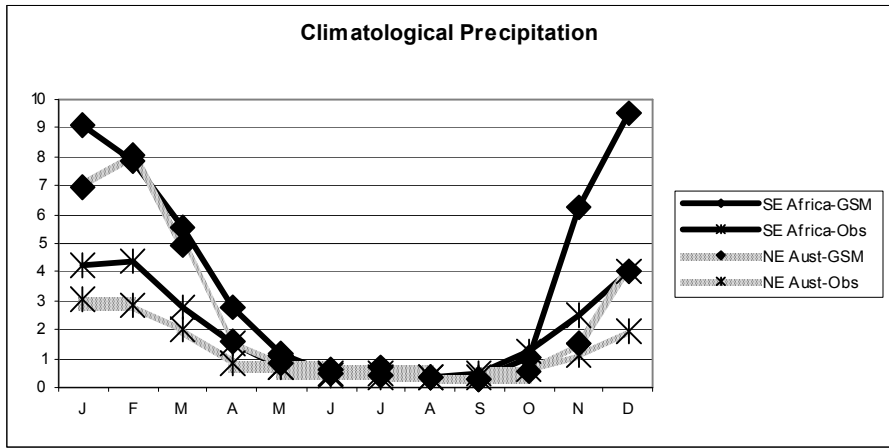


Figure 7: The climatological (1961-1990) annual cycle of precipitation for the ECPC SFM (GSM) and CRU observations (Obs) in kg/m²/day.

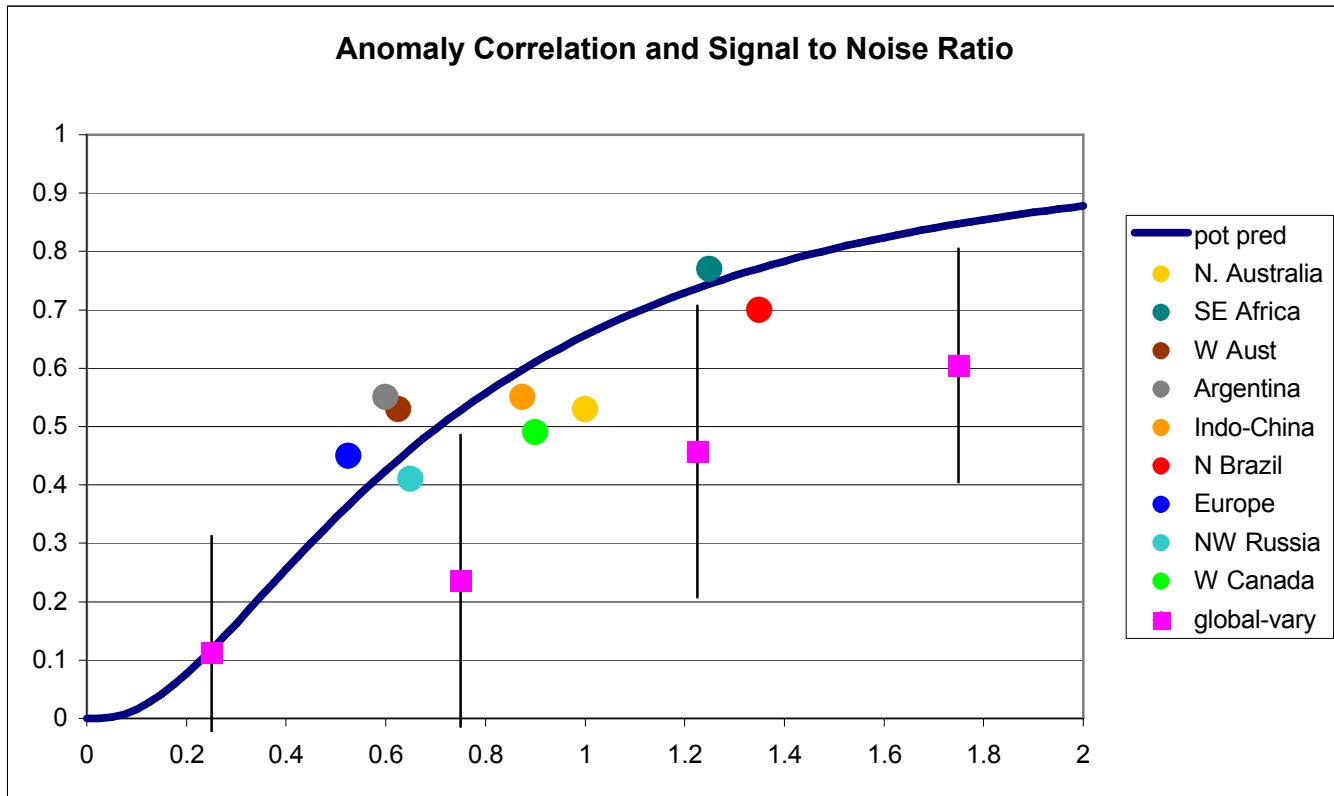


Figure 8: Anomaly correlation (y-axis) plotted against the signal to noise ratio (x-axis). The solid line is the theoretical relationship between the two (potential predictability), the pink squares show the binned global average with error bars, and the colored circles show the regions discussed in the text.